Applied Surface Science 567 (2021) 150802

Contents lists available at ScienceDirect

Applied Surface Science

journal homepage: www.elsevier.com/locate/apsusc

Full Length Article

Experimental tuning of AuAg nanoalloy plasmon resonances assisted by machine learning method

Robert Kozioł [a], Marcin Łapiński [a], Paweł Syty [b], Wojciech Sadowski [a], Józef E. Sienkiewicz [b], Bartosz Nurek [a], Valentin Adrian Maraloiu [c], Barbara Kościelska [a,*]

[a] Institute of Nanotechnology and Materials Engineering, Faculty of Applied Physics and Mathematics, Gdańsk University of Technology, ul. Gabriela Narutowicza 11/12, 80-233 Gdańsk, Poland

[b] Institute of Physics and Computer Science, Faculty of Applied Physics and Mathematics, Gdańsk University of Technology, ul. Gabriela Narutowicza 11/12, 80-233 Gdańsk, Poland

[c] National Institute of Materials Physics, 077125 Magurele, Ilfov, Romania

ARTICLE INFO

Keywords:
Bimetallic alloyed nanostructures
Dewetting
Plasmon resonance
Artificial neural network

ABSTRACT

Plasmonic nanostructures based on AuAg nanoalloys were fabricated by thermal annealing of metallic films in an argon atmosphere. The nanoalloys were chosen because they can extend the wavelength range in which plasmon resonance occurs and thus allow the design of plasmonic platforms with the desired parameters. The influence of initial fabrication parameters and experimental conditions on the formation of nanostructures was investigated. For the surface morphology studies, chemical composition analysis and nanograin structure, Scanning Electron Microscopy (SEM), X-Ray Photoelectron Spectroscopy (XPS), Energy Dispersive X-Ray Spectroscopy (EDS) and High-Resolution Transmission Electron Microscopy (HR TEM) measurements were performed. The position of the resonance band was successfully tuned in the 100 nm range. The EDS together with the XPS analysis confirmed the formation of an alloy with the aspect ratio of individual metals in a single nanoisland similar to the ratio of the thicknesses of the initially sputtered layers. The experimental research was complemented by the neural network model, which enables the calculation of the absorbance peak depending on the thickness of Au and Ag layers and the annealing time. The proposed model of machine learning makes it possible to fine-tune the desired position of the plasmon resonance.

1. Introduction

Metallic nanoparticles have been attracting the attention of scientists for over a decade. It is caused by their unique catalytic and optical properties. In particular, collective oscillations of conductive electrons, known as localised surface plasmon resonance (LSPR), enable many applications in various fields, such as photocatalysis [1,2], photovoltaic devices [3,4], surface-enhanced Raman scattering [5,6] and even anti-cancer therapy [7]. This group includes bimetallic nanoparticles, which are currently very popular. They are nanomaterials composed of two different metal elements. Their uniqueness is evidenced by the attributes that are typically a combination of properties derived from metal amalgams [8]. These properties, and thus applicability of such nanoparticles, are related not only to their size and shape, as in the case of monometallic nanoparticles, but also to their chemical composition and structure [6,9–11]. Hence, proper control over the fabrication of such systems poses a significant experimental challenge.

In the case of bimetallic materials, noble metals play a key role. Due to full filled d-orbitals and relatively low cohesive energy, gold and silver nanoalloys are mainly investigated [12]. Their resonance band typically occurs at wavelengths around 420 and 530 nm for Ag and Au, respectively [13]. In addition, from an optical properties point of view, Ag is distinguished by the largest extinction cross section, but on the other hand, its LSPR application is restricted by poor chemical stability and low corrosion resistance [13,14]. Au, in turn, apart from being an effective plasmonic material, is distinguished by physical and chemical stability [15]. Due to alloying of these metals, the synergistic effects induced by the hetero-junction charge transfer between them not only solve the problem of Ag corrosion but also make it possible to tune the LSPR frequency in the range from 420 to 530 nm [16,17].

Since physical and chemical properties of these nanoalloys are composition and order-dependent, a complete understanding of the

* Corresponding author.
E-mail address: barbara.koscielska@pg.edu.pl (B. Kościelska).

https://doi.org/10.1016/j.apsusc.2021.150802
Received 21 April 2021; Received in revised form 24 June 2021; Accepted 28 July 2021
Available online 2 August 2021

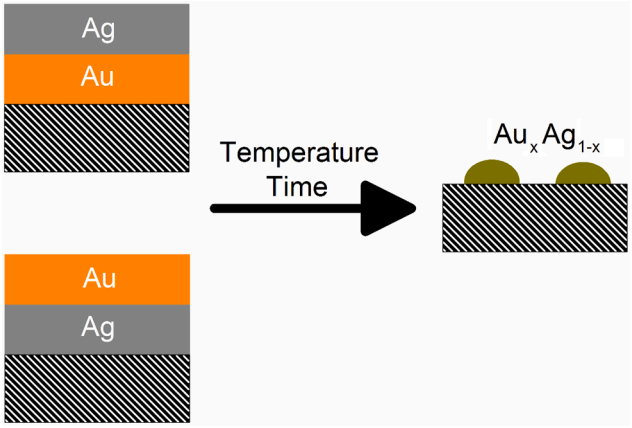

Fig. 1. Schematic illustration of the fabrication process of alloy nanostructures.

mechanisms involved in fabrication is essential to gain full control over the fabrication of desired nanostructures. For this purpose, a phase diagram is required [18]. However, in the nanoscale regime, where the number of atoms is very small, alloys cannot be described by classical thermodynamics. As a perfect complement to the experimental kinetic considerations, many efforts have been made to find an extension of classical theory to the nanoscale, which gave rise to a new interdisciplinary theory named nanothermodynamics [19]. Its advantage over other predictive methods, such as Metropolis Monte Carlo or Molecular Dynamics results from the possibility predicting phase diagrams of alloys in the entire composition range, which in turn translates into solving some fundamental problems concerning the behaviour of nanoalloys [20,21].

The ability to control the position of the plasmon resonance seems to be the most important reason for creating nanoalloy plasmonic platforms. Such platforms may find application in a wide range of nanosensors operating in a wide frequency range. Of course, the best solution would be to include artificial neural networks (ANN) in their design.

In recent years, artificial neural networks have found applications in various engineering problems. ANN, as an alternative to classical approaches using of continuum mechanics, are computer models that are able to show dependence of free parameters on responses obtained from the external environment [22,23]. Since each of the multiple fabrication parameters used to control the process of the formation of alloy nanostructures has an immense influence on the optical properties of the obtained structure [24], ANN can be extremely useful not only to present the influence of each parameter on the obtained results, but also to

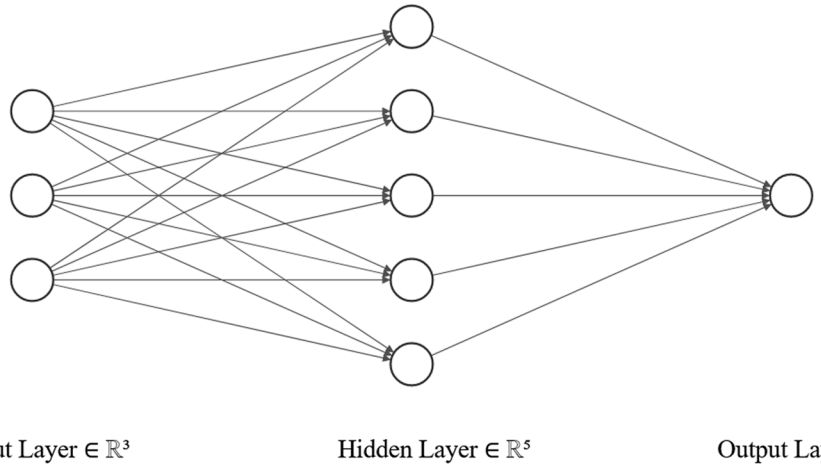

Fig. 2. Topology of the neural network used to build the model (3–5–1), with the activation functions of the hyperbolic tangent and sigmoid in the hidden and output layers, respectively.

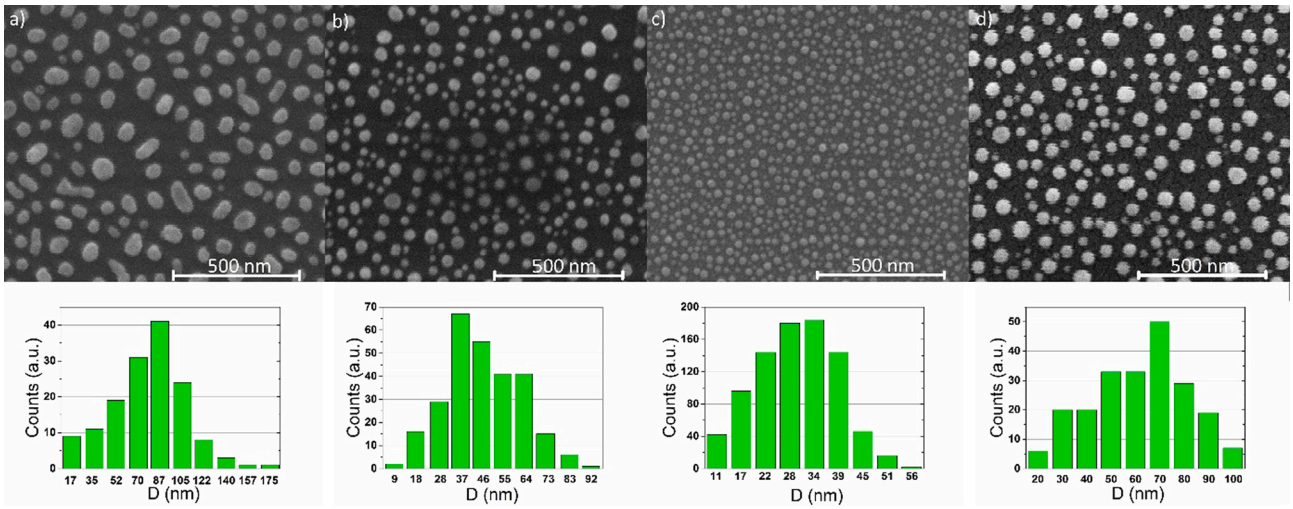

Fig. 3. *SEM pictures of nanostructures resulting from annealing at 550 °C for 15* min*: Au (2.8 nm) / Ag (2.8 nm) bilayer (a); Au (2.8 nm) monolayer (b); Ag (2.8 nm) monolayer (c) and Ag (2.8 nm) / Au (2.8 nm) bilayer (d).*

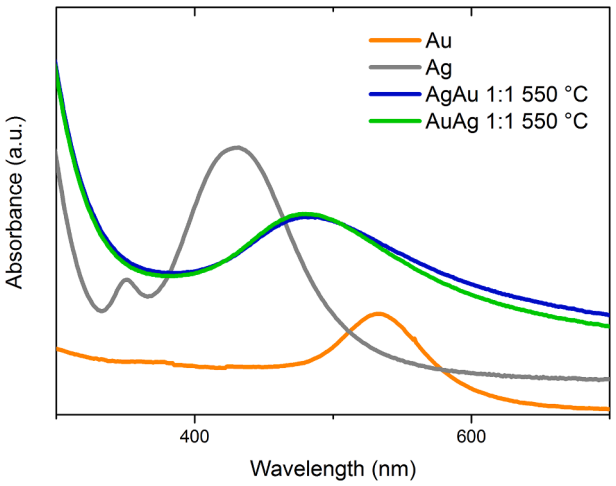

Fig. 4. *UV–Vis spectra of nanostructures resulting from annealing at 550 °C for 15 min: Au (2.8 nm) / Ag (2.8 nm) bilayer (a); Au (2.8 nm) monolayer (b); Ag (2.8 nm) monolayer (c) and Ag (2.8 nm) / Au (2.8 nm) bilayer (d).*

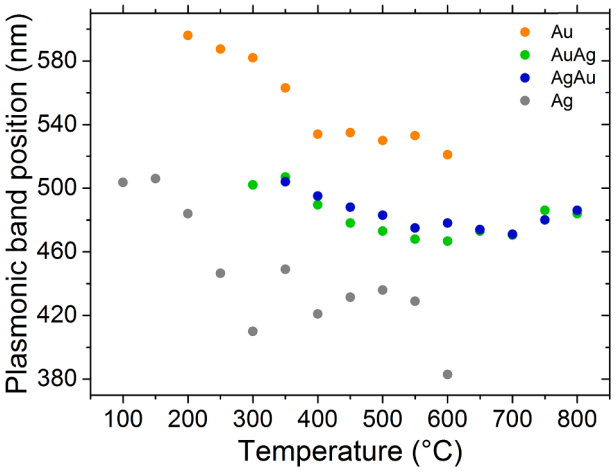

Fig. 5. The influence of annealing temperature on the position of plasmon resonance for the nanostructures grown from: Au (2.8 nm) monolayer (orange dots); Au (2.8 nm) / Ag (2.8 nm) bilayer (green dots); Ag (2.8 nm) / Au (2.8 nm) bilayer (blue dots) and Ag (2.8 nm) monolayer (grey dots).

provide a specific set of fabrication parameters needed for obtaining structures with specific properties.

This work is devoted to designing plasmonic platforms based on the AuAg nanoalloy. In addition to how to produce them and study their structure, we would also like to show the effects of using artificial neural networks to predict the location of plasmon resonance. The position of the single peak shown in the plasmon resonance of the Au-Ag alloy nanoparticle system does not correspond to any peaks of the pure metal components. Then, starting from the position of the pure Ag layer resonance peaks, they are shifted to longer wavelengths at increased Au concentration. Obviously, this relationship is true when we consider nanoparticles of the same size and shape. If we additionally take into account the size of the nanostructures and their shape, the position of the plasmon resonance peak may change regardless of the mutual ratio of the amount of metals making up the nanoalloys. We intend to prove that changing the experimental parameters such as Au and Ag layer thickness and annealing time allows the optical spectra to be controlled. The collected experimental data is used to build a neural network model, which is used to adjust the experimental parameters to the desired plasmon resonance position. In other words, if we ask "the machine" a

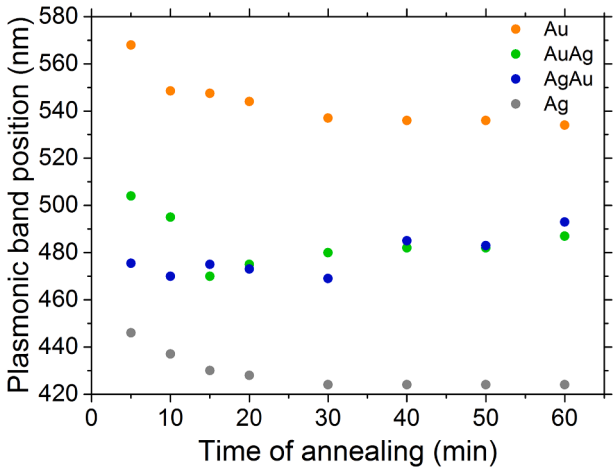

Fig. 6. *The influence of annealing time on the position of plasmon resonance for nanostructures grown from: Au (2.8 nm) monolayer (orange dots) Au (2.8 nm) / Ag (2.8 nm) bilayer (green dots); Ag (2.8 nm) / Au (2.8 nm) bilayer (blue dots) and Ag (2.8 nm) monolayer (grey dots). The annealing temperature is 550 °C.*

question about how to produce a sample that would lead to plasmon resonance at a particular wavelength, we should get an answer both in terms of the mutual ratio of initial layer thicknesses, as well as thermal conditions and the time in which the layers should be annealed.

2. Materials and methods

Glass and Si substrates were used for deposition of gold/silver layers. The substrates were cleaned with acetylacetone and then rinsed with ethanol. Thin Au and Ag layers were sputtered using a table-top dc magnetron sputtering coater (EM SCD 500, Leica) in the pure Ar plasma state (Argon, Air products 99,999%). Both Au and Ag targets were 99,99% pure. The coating process was carried out with a deposition rate of about 0.4 nm per second and an incident power in the range of 30–40 W. The sputtering system was equipped with a quartz crystal microbalance for in situ film thickness measurements. The prepared layers were put into a hot furnace and annealed in argon atmosphere at various temperatures in the range of 300–800 °C and time conditions (from 5 to 60 min) in order to produce nanostructures, as schematically presented in Fig. 1. The structures of AuAg nanoalloys were prepared by sequential sputtering of metal thin layers (Au/Ag or Ag/Au) followed by annealing under various conditions in an argon atmosphere. The basic single layer thickness was usually 2.8 nm, which was again selected based on our previous studies of Au and Ag metallic nanostructures [25,26]. However, in order to find out how the individual nanograins are formed and whether they are homogeneous (and made of Au_xAg_y alloy), the initial thickness ratio of the Au and Ag layers was also changed (in addition to changing the order in which they were applied). For the structural studies, samples consisting of triple layers, Au/Ag/Au and Ag/Au/Ag were also prepared. In the first step, 550 °C was chosen as the temperature for manufacturing AuAg nanoalloys, in which it was possible to obtain Au and Ag nanostructures giving high-intensity plasmon resonance [25,26].

A FEI Quanta FEG 250 Scanning Electron Microscope (SEM) operating at 10 kV was used to analyse the surface morphology of the samples. The analytical Transmission Electron Microscopy (TEM) investigations were performed on a JOEL JEM ARM 200F HR TEM apparatus equipped with an EDS detector. For nanograin structure and chemical composition, several TEM techniques were used, including conventional and High-Resolution imaging (TEM/HRTEM), Selected-Area Electron Diffraction (SAED), EDS and Scanning Transmission Electron Microscopy (STEM). SEM and TEM experiments were carried out on samples deposited on silicon substrates.

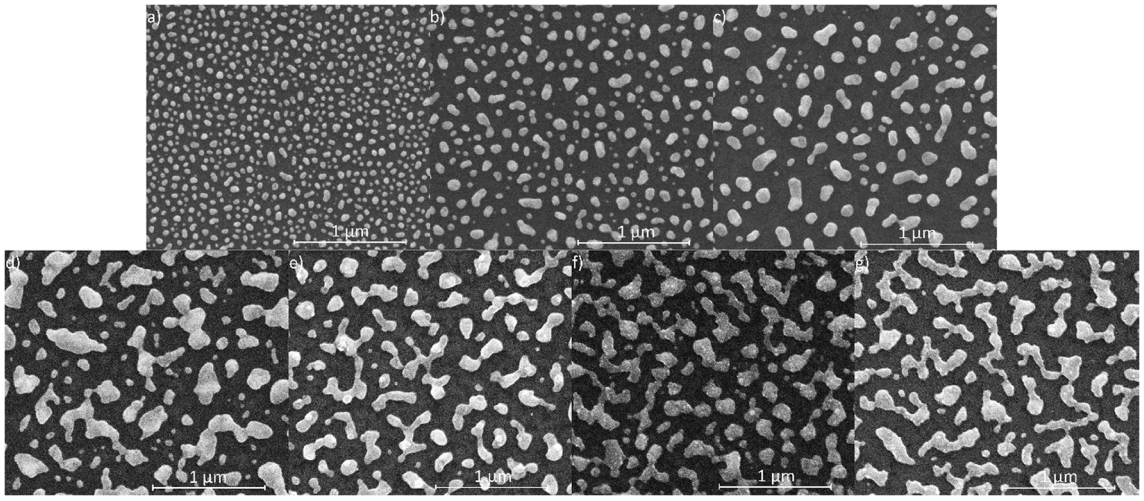

Fig. 7. *SEM images of nanostructures formed by annealing at 550 °C for 15 min of bilayers. The first layer is Au with the same thickness of 2.8 nm, the second is Ag with a thickness of (a) 2 nm, (b) 3 nm, (c) 4 nm, (d) 5 nm (e) 6 nm, (f) 7 nm and (g) 8 nm.*

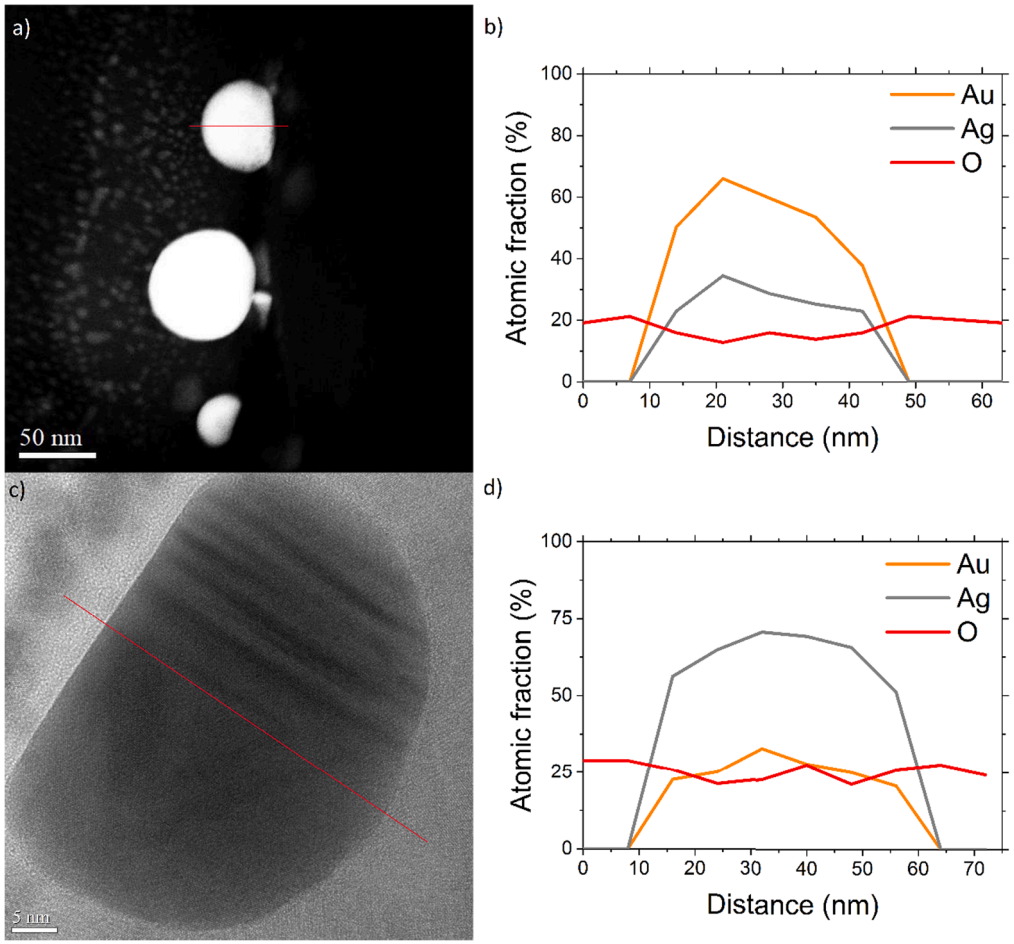

Fig. 8. HR TEM image of a cross section of a nanoisland made of sandwich-type structure with a total thickness of 6 nm with a detailed EDS analysis of the cross section of the presented nanoislands. Au/Ag/Au configuration (a, b), Ag/Au/Ag configuration (c, d), annealed at 550 °C for 15 min.

UV–vis spectra were recorded with a Thermo Fisher Scientific Evolution 220 double beam spectrophotometer in the absorbance mode, in the range of 200 nm–1100 nm. These measurements were carried out on samples deposited on glass substrates.

The quality of the obtained nanostructures and electron states of atoms in the AuAg nanoalloy were measured using X-ray photoelectron spectroscopy (XPS), an Omicron NanoTechnology spectrometer with a 128-channel collector. XPS measurements were performed at room temperature under a ultra-high vacuum conditions, around 10^{-9} mBar. The photoelectrons were excited by an Mg-Kα X-Ray source. The X-ray anode was operated at 15 keV and 300 W. The Omicron Argus hemispherical electron analyser with a round aperture of 4 mm was used for

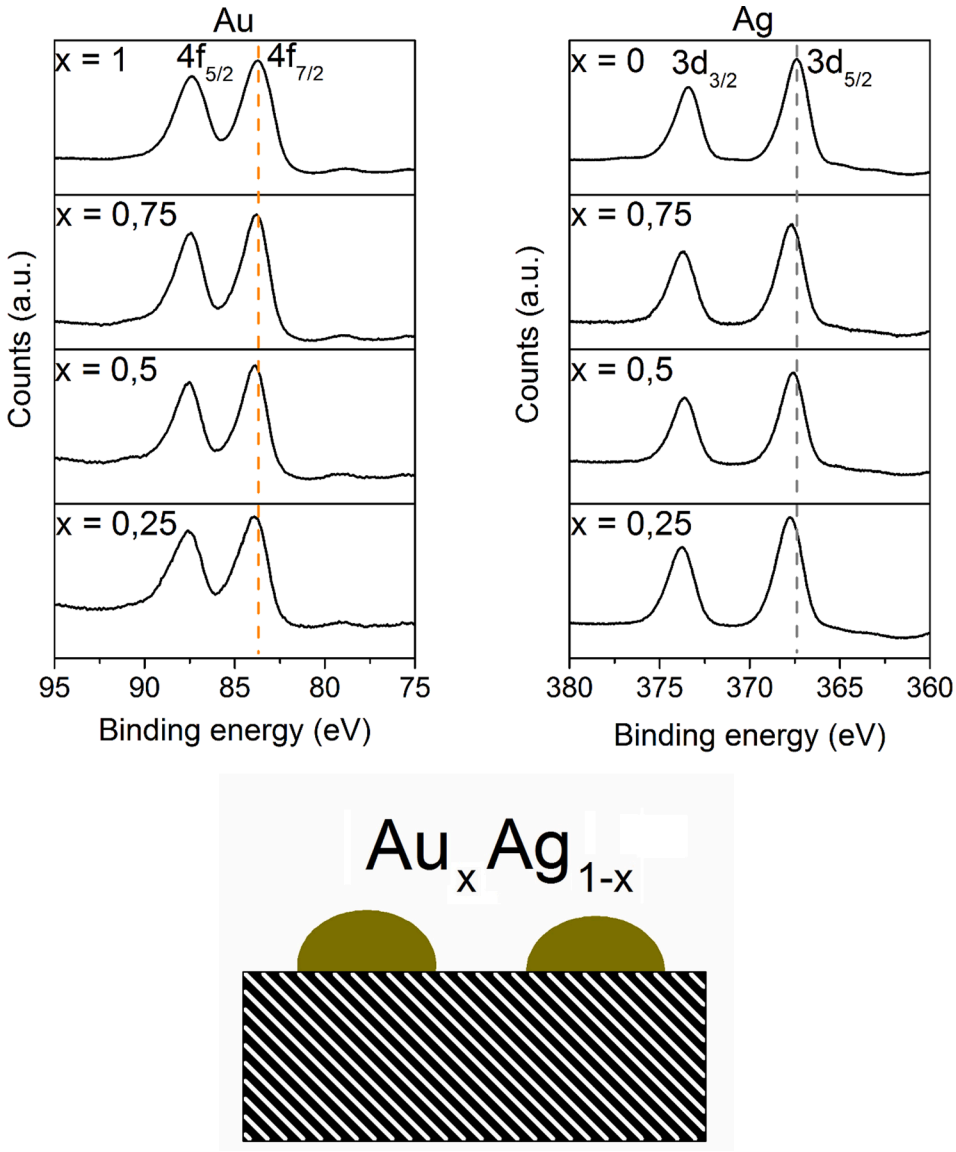

Fig. 9. XPS spectra of 4f Au and 3d Ag regions of the samples (top) and the schematic view of nanostructures (bottom). Every measured structure was achieved either from a single layer or bilayers with an Ag layer sputtered on top of an Au layer. The total thickness of such systems was 6 nm. The samples prepared in this way were then annealed at 550 °C for 15 min.

the analysis of the emitted photoelectrons. The binding energies were corrected using the background C1s line (285.0 eV). XPS spectra were analysed with Casa-XPS software using Shirley background subtraction and Gaussian–Lorentzian curve as the fitting algorithm.

In addition, a predictive numerical model based on machine learning was proposed. Its main purpose was to estimate the positions of the resonance peaks for a given annealing time and thickness of Au/Ag layers, for which no experimental data was collected. The model was built using the multi-layer, fully-connected, one-directional artificial neural network [27] and trained using the available experimental data (31 data points: annealing time, Au and Ag layer thickness as inputs, and peak resonance as output). The complete data set used for creating the predictive model is available to download at [28]. The topology of the neural network is presented in Fig. 2. The number of neurons in the input (3) and output (1) layers corresponds to the number of input and output parameters, respectively. The number of hidden layers, as well as the activation functions (hyperbolic tangent in the hidden layer, and sigmoid in the output layer) were chosen experimentally to give the best overall results (minimize prediction errors on validation data).

To train the neural network, the Adam learning algorithm [29] and the root mean square error (RMSE) as a loss function were used. To avoid overfitting the model, the k-fold (k = 10) cross-validation procedure [30] was applied: the entire data set was randomly divided into 10 parts, each consisting of (different) 28 training and 3 validating data points, which gave 10 different models. The method allowed to reduce the size of the validation data set in each model, which was important when the amount of data was limited [31]. The models were independently trained using the training data points, while the validating ones were used to control the training process. Trained models were benchmarked according to RMSE on validation data. The final predictive model was built by averaging the results from the above 10 models. All experimental data used for for machine learning model training (UV–vis spectra and SEM images), along with a list of all samples, are available at [28].

3. Results and discussion

Fig. 3 presents exemplary SEM images of nanostructures formed as a result of annealing of Au/Ag (Fig. 3a) and Ag/Au (Fig. 3d) layers with a thickness of 2.8 nm each, at the 550 °C for 15 min. For comparison, SEM

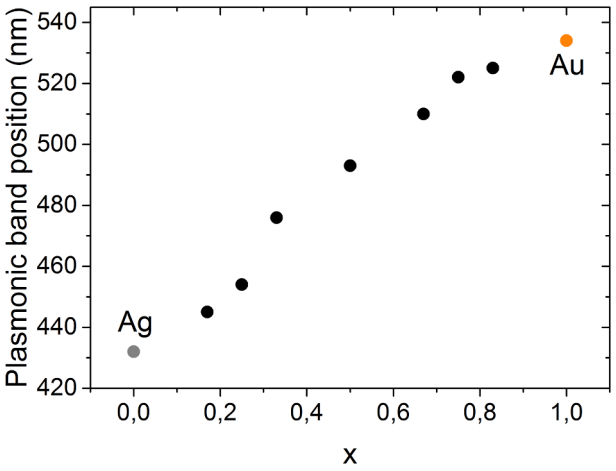

Fig. 10. Position of the plasmonic band of Au_xAg_{1-x} nanoalloy structures depending on the initial Au/Ag composition. Every measured structure was achieved either from a single layer or bilayers with an Ag layer sputtered on top of an Au layer. The total thickness of such systems was 6 nm. The samples prepared in this way were then annealed at 550 °C for 15 min.

images of Au (Fig. 3b) and Ag (Fig. 3c) nanostructures made of Au and Ag films with thicknesses of 2.8 nm were added.

Comparing Fig. 3a and Fig. 3d, it can be concluded, that the nanostructures differ in both the average size and shape, which certainly affects their plasmonic properties. As is well known, the UV–vis spectrum of metallic nanostructures can be influenced by many factors, such as the size, shape on nanostructures and the dielectric properties of surrounding medium. For instance, their elongated shape may result in an additional maximum in the UV spectrum [32–37]. The maxima of plasmon resonance of the nanostructures shown in Fig. 3 are respectively: 470 nm (a), 550 nm (b), 430 nm (c) and 475 nm (d), as presented in Fig. 4.

As can be seen, there is not much difference between the resonance position of nanoalloys grown from films deposited in different configurations: Au/Ag and Ag/Au. Both resonances are located between the values characterizing pure Au and Ag. However, the resonance peak from nanoalloys is not as sharp as that from Au or Ag. The influence of the annealing temperature on the position of the plasmon resonance is shown in Fig. 5. Of course, it should be noted that both lowering the temperature in relation to the selected 550 °C, and increasing it, change the shape of nanostructures, similarly to the changes observed in monolayers [25,26].

It can be concluded that if the position of the plasmon resonance is taken as the reference parameter, then the sequence of the layers has no effect on the formation of nanoalloy. It is obvious, of course, that metals willingly form alloys, but on the other hand, we are dealing with thin layers in which the melting point strongly depends on their thickness. Among the solid configurations that can be potentially obtained from such layer systems, archetypically are either a core–shell, a fully segregated, so-called Janus-like or a fully mixed alloy [38]. However, it is well known that Au and Ag atoms begin to inter-diffuse at temperature as low as 100 °C [39]. It is quite straightforward to define what type of structure is achieved from their optical properties. Namely, in the case of the formation fully mixed nanoalloys, a single absorption peak is observed, while in completely separated phases, i.e. the core–shell structure, two characteristic absorption peaks appear [40].

The influence of the annealing time on the position of the resonance peak was also investigated. The results are shown in Fig. 6. 550 °C was again selected as the annealing temperature. Again, the conclusion is that there are no major differences between the samples obtained as a result of annealing of Au/Ag and Ag/Au bilayers. Anyway, in the selected interval, the annealing time seems to have little influence on the position of the plasmon resonance also for monolayers. However, the very formation of nanoalloys in the form of nanostructures is interesting. Fig. 7 shows SEM images of nanostructures formed by annealing at 550 °C for 15 min of bilayers, in which the first layer was Au with the same thickness of 2.8 nm, and the thickness of the Ag layer deposited thereon increased.

We believe that the annealing conditions are not suitable for such selected layers, however, as can be seen with a silver layer thickness of 6 nm, a single nanostructure appears to form from smaller ones. To say more about the formation of nanoalloys, layers of different initial thicknesses as well as Au/Ag/Au and Ag/Au/Ag multilayers were proposed for annealing. TEM images of samples prepared in this way are shown in Fig. 8.

Each film from which presented nanostructures were made was 2 nm thick. Therefore, the thickness of the multilayer system was 6 nm in total, with aspect ratios Au to Ag 2:1 (Fig. 8a, b) and 1:2 (Fig. 8c, d). As can be seen, obtained nanoislands are homogeneous, which suggests alloy formation rather than fully separated type structures. Detailed EDS analysis of the nanoisland cross-section is presented in Fig. 8b and 8d. Interestingly, the aspect ratio of individual metals in a single nanoisland is similar to the ratio of thicknesses of the sputtered layers before annealing.

The structure of the samples was also examined using the XPS method. The high-resolution spectra of 4f Au and 3d Ag regions are presented in Fig. 9.

As can be seen, both the Au 4f and Ag 3d spectra consist of two peaks, forming doublets. The Au $4f_{7/2}$ and Ag $3d_{5/2}$ peaks are shifting relative to the pure metal peak towards higher energies. Changes in the Au peak position are usually dependent on the size of the cluster, cluster–substrate interaction, cluster morphology, or a change the environment of atoms [41,42]. Also, the shift of Ag peak can be attributed to the modified electronic structure [43]. This shift of Au 4f and Ag 3d peaks in gold-silver systems was noticed by others and explained as a partial charge transfer between atoms [44–46]. Moreover, it should be noted that the peaks characteristic of Ag–O compounds were not observed in the XPS spectra, which is consistent with the EDS results.

The idea behind the creation of such alloy plasmonic platforms was to obtain synergistic effects of the combined properties of metals, which should result in the possibility of tuning optical properties of such systems. As shown in Fig. 10, which presents the dependence of the plasmonic band position on the gold content, a linear trend is achieved. However, it should be emphasized that such a linear trend applies only to samples with the same initial thickness (6 nm), annealed under the same conditions (550 °C for 15 min). This trend can be a great tool for fine-tuning the operating range of nanosensors. For this purpose, an artificial neural network was used. In order to build a reliable model, it was necessary to take into account a much wider spectrum of samples than those whose resonance positions are presented in Fig. 10. Of course, the results obtained from the model should be consistent with the experiment also in the linear fit shown in Fig. 10.

For each model, the independent training of the neural network was successfully completed after 100,000 – 500,000 epochs, in the sense of minimizing the loss function (RMSE) on the validating data set. The RMSE for these trained models ranged from 1.66 nm to 5.26 nm. The final predictive model was constructed as a weighted average of all models, with the weights selected as 1/RMSE. The RMSE (on the complete dataset) of this averaged model was found to be 1.53 nm, which is lower than that for any of the individual models alone. Using this model, we are able to estimate the positions of the absorption maxima (resonance peaks) for the given annealing times, as well as the thicknesses Au and Ag layers, with minimized risk of overfitting. Example of the results of such predictions for selected annealing times are shown in Fig. 11. A few numerical results for different (randomly selected) combinations of input parameters are collected in Table 1. Let us note that these results are *predictions* only, based on the available experimental data. But, since the predictive model has been trained using the cross-validation

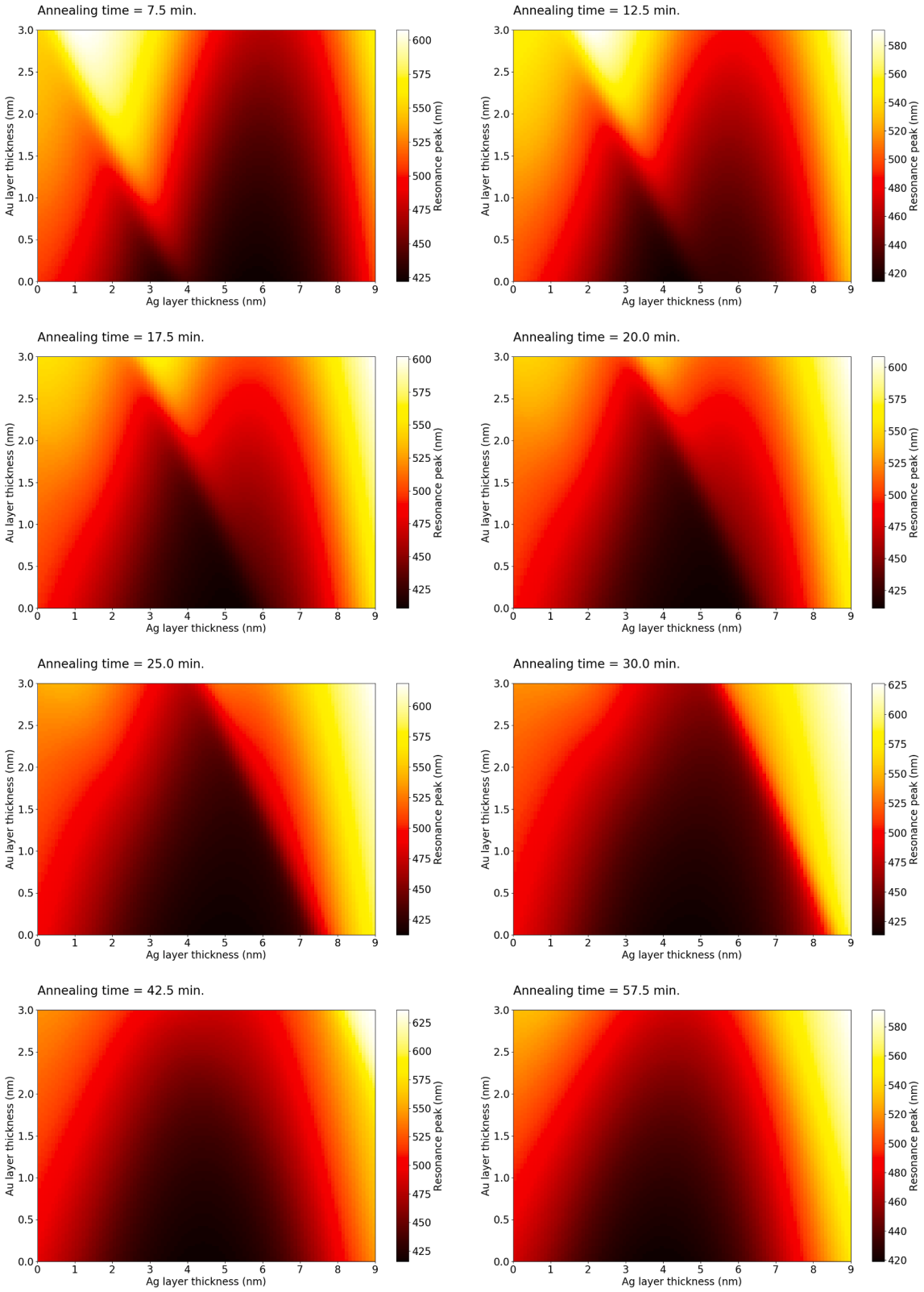

Fig. 11. Machine predictions of the absorption maxima positions as a function of Au and Ag layer thickness for several annealing times.

method, we believe that the error should not exceed 1.53 nm (the final RMSE).

Since the source experimental data [28] covered the range 5–60 min of annealing time, 0–2.8 nm of Au layer thickness and 0–8.4 nm of Ag layer thickness and due to data normalization, it should be also noted that the most reliable in a given range of input parameters, e.g. for annealing times from 5 to 60 min, Au layer thickness from 0 to 3 nm, and Au layer thickness from 0 to 9 nm. In addition, the accuracy of the model is limited by the relatively small amount of training data. However, when new (or more accurate) experimental data becomes available, the

Table 1
Machine predictions of the positions of the absorption maxima as a function of Au and Ag layer thickness for several combinations of input parameters, that were not used in the experiment.

Annealing time (min)	Au layer thickness (nm)	Ag layer thickness (nm)	Predicted resonance peak (nm)
25	2.0	0.0	519.88
35	2.5	0.0	529.86
25	0.0	3.0	424.03
45	2.0	5.0	450.22
35	2.5	8.0	610.09
35	2.0	4.0	448.85
35	1.0	2.0	484.51
12	2.0	6.0	458.92

model can be easily fine-tuned using the transfer-learning procedure [47].

The training dataset [28] includes a few specific cases where the positions of resonance peak were located above 600 nm, mainly due to the large size of the grains in the resulting alloy. As a consequence, the predictive model is also able to give predictions above 600 nm, but – as one read from Fig. 11 – this might occur only for very specific combinations of input parameters, which are visualized by the most bright parts of the pictures (one of that combination is presented in Table 1). There is a possibility to train a new model, excluding these specific cases, but it would be limited to the narrower range of input parameters. In the present work we decided to leave the full training dataset, keeping the predictive model more general.

4. Conclusions

This work presents the synthesis of plasmonic platforms based on AuAg nanoalloy with the use of a time-saving and cost-effective method. The influence of initial fabrication parameters i.e. annealing time and temperature, as well as the configuration and thicknesses ratio of the sputtered layers, was investigated. Due to fabrication in the argon atmosphere, there was no corrosion of the silver, hence no major differences between the different layers ordering were observed. As shown, the combination of these two metals made it possible to tune the LSPR over the 100 nm range with a linear dependence on the Au content in the plasmonic platform. It has been presented that in the plasmonic platform fabrication regime, artificial neural networks can be successfully used to determine the initial fabrication parameters needed for the LSPR between the experimental results. The ability to fine-tune the position of the resonant peak along with quick information about the fabrication parameters needed for such a procedure creates exceptional opportunities in the design of highly sensitive sensors.

Our studies have shown that changes in the composition and annealing over time of AuAg alloys with an appropriate neural network model can be used to efficiently tune plasmon resonance. This property of AuAg nanoalloys can be applied in various types of sensors, surface spectroscopy, and optoelectronics.

CRediT authorship contribution statement

Robert Kozioł: Visualization, Resources, Investigation, Writing – original draft. **Marcin Łapiński:** Investigation, Formal analysis, Methodology. **Paweł Syty:** Formal analysis, Software, Visualization, Writing – original draft. **Wojciech Sadowski:** Formal analysis, Conceptualization, Validation. **Józef E. Sienkiewicz:** Validation, Formal analysis. **Bartosz Nurek:** Resources. **Valentin Adrian Maraloiu:** Investigation. **Barbara Kościelska:** Conceptualization, Supervision, Project administration, Writing - review & editing.

Declaration of Competing Interest

The authors declare that they have no known competing financial interests or personal relationships that could have appeared to influence the work reported in this paper.

Acknowledgements

MŁ and RK acknowledge the CERIC-ERIC Consortium for the access to experimental facilities (HR-TEM microscope) and the financial support (project no 20187051).

References

[1] S. Manchala, L.R. Nagappagari, S.M. Venkatakrishnan, V. Shanker, Solar-Light Harvesting Bimetallic Ag/Au Decorated graphene Plasmonic System with Efficient Photoelectrochemical Performance for the Enhanced Water Redution Process, ACS Appl. Nano. Mater. 2 (2019) 4782–4792, https://doi.org/10.1021/acsanm.9b00684.
[2] S. Zhang, M. Li, J. Zhao, H. Wang, X. Zhu, J. Han, X. Liu, Plasmonic AuPd-based Mott-Shottky photocatalyst for synergistically enhanced hydrogen evolution from formic acid and aldehyde, App. Catalisys B: Environ. 252 (2019) 24–32, https://doi.org/10.1016/j.apcatb.2019.04.013.
[3] S. Saravanan, R. Kato, M. Balamurugan, S. Kaushik, T. Soga, Efficiency improvement in dye sensitized solar cells by the plasmonic effect of green synthesized silver nanoparticles, J. Sci.: Adv. Mater. Devices 2 (2017) 418–424, https://doi.org/10.1016/j.jsamd.2017.10.004.
[4] M.A.K.L. Dissanayake, J.M.K.W. Kumari, G.K.R. Senadeera, C.A. Thotawatthage, Efficiency enhancement in plasmonic dye-sensitized solar cells with TiO_2 photoanodes incorporating gold and silver nanoparticles, J. Appl. Electrochem. 46 (2016) 47–58, https://doi.org/10.1007/s10800-015-0886-0.
[5] M. Fan, F.-J. Lai, H.-L. Chou, W.-T. Lu, B.-J. Hwang, A.G. Brolo, Surfance-enhanced Raman scattering (SERS) from Au: Ag bimetallic nanoparticles: the effect of the molecular probe, Chem. Sci. 4 (2013) 509, https://doi.org/10.1039/c2sc21191b.
[6] J.F. Sánchez-Ramírez, U. Pal, L. Nolasco-Hernández, J. Mendoza-Álvarez, J. A. Pescador-Rojas, Synthesis and Optical Properties of Au-Ag Alloy Nanoclusters with Controlled Composition, J. Nanomater. (2008) 1–9, https://doi.org/10.1155/2008/620412.
[7] E.R. Evans, P. Bugga, V. Asthana, R. Drezek, Metallic nanoparticles for cancer immunotheraphy, Mater. Today 21 (2018) 673–685, https://doi.org/10.1016/j.mattod.2017.11.022.
[8] P. Srinoi, Y.-T. Chen, V. Vittur, M.D. Marquez, T.R. Lee, Bimetallic Nanoparticles: Enhanced Magnetic and Optical Properties for Emerging Biological Applications, Appl. Sci. 8 (2018) 1106, https://doi.org/10.3390/app8071106.
[9] G. Qiu, S.P. Ng, L. Wu, Bimetallic Au-Ag alloy nanoislands for highly sensitive localized surface plasmon resonance biosensing, Sens. Actuators, B 265 (2018) 459–467, https://doi.org/10.1016/j.snb.2018.03.066.
[10] J. Zhang, Y. Lou, H. Zhou, Y. Zhao, Z. Wang, L. Shi, S. Yuan, Electrodeposited AgAu nanoalloy enhancing photoelectric conversion efficiency of dye sensitized solar cells, Electrochmica. Acta. 324 (2019), 134858, https://doi.org/10.1016/j.electacta.2019.134858.
[11] R. Ferrando, Structure and Properties of Nanoalloys, Frontiers Nanosciece (10) (2016) 2–337. ISBN: 978-0-08-100212-4.
[12] G. Guisbiers, R. Mendoza-Cruz, L. Bazán-Díaz, J.J. Velázquez-Salazar, R. Mendoza-Perez, J.A. Robledo-Torres, J.-L. Rodriguez-Lopez, J.M. Montejano-Carrizales, R. L. Whetten, M. José-Yacamán, Electrum, the Gold-Silver Alloy, from the Bulk Scale to the Nanoscale: Synthesis Properties, and Segregation Rules, ACS Nano. 10 (1) (2016) 188–198, https://doi.org/10.1021/acsnano.5b05755.
[13] M.A. Garcia, Corrigendum: Surface plasmons in metallic nanoparticles: fundamentals and applications, J. Phys. D: Appl. Phys. 44 (2011), 283001 stacks.iop.org/JPhysD/45/389501.
[14] L. Guo, J.A. Jackman, H.-H. Yang, P. Chen, N.-J. Cho, D.-H. Kim, Strategies for enhancing the sensitivity of plasmonic nanosensors, Nano. Today 10 (2015) 213–239, https://doi.org/10.1016/j.nantod.2015.02.007.
[15] A. Liu, G. Wang, F. Wang, Y. Zhang, Gold nanostructures with near-infrared plasmonic resonance: Synthesis and surface functionalization, Coord. Chem. Rev. 336 (2017) 28–42, https://doi.org/10.1016/j.ccr.2016.12.019.
[16] C. Gao, Y. Hu, M. Wang, M. Chi, Y. Yin, Fully Alloyed Ag/Au Nanospheres: Combining the Plasmonic Property of Ag with the Stability of Au, J. Am. Chem. Soc. 136 (20) (2014) 7474–7479, https://doi.org/10.1021/ja502890c.
[17] S. Liu, G. Chen, P.N. Prasad, M.T. Swihart, Synthesis of Monodisperse Au, Ag, and Au-Ag Alloy Nanoparticles with Tunable Size and Surface Plasmon Resonance Frequency, Chem. Mater. 23 (18) (2011) 4098–4101, https://doi.org/10.1021/cm201343k.
[18] Y.A. Chang, S. Chen, F. Zhang, X. Yan, F. Xie, R. Shmid-Fetzer, W.A. Oates, Phase diagram calculation: past, present and future, Prog. Mater Sci. 49 (2004) 313–345, https://doi.org/10.1016/S0079-6425(03)00025-2.
[19] C.C. Yang, Y.-W. Mai, Thermodynamics at the nanoscale: A new approach to the investigation of unique physicochemical properties of nanomaterials, Mater. Sci. Eng.: R: Reports 79 (2014) 1–40, https://doi.org/10.1016/j.mser.2014.02.001.
[20] Grégory Guisbiers, Sergio Mejia-Rosales, Subarna Khanal, Francisco Ruiz-Zepeda, Robert L. Whetten, Miguel José-Yacaman, Gold−Copper Nano-Alloy, "Tumbaga",

in the Era of Nano: Phase Diagram and Segregation, Nano Lett. 14 (2014) 6718–6726, https://doi.org/10.1021/nl503584q.
[21] L. Delfour, J. Creuze, B. Legrand, Exotic Behavior of the Outer Shell of Bimetallic Nanoalloys, Phys. Rev. Lett. 103 (2009), https://doi.org/10.1103/PhysRevLett.103.205701.
[22] Marcus Stoffel, Rutwik Gulakala, Franz Bamer, Bernd Markert, Artificial neural networks in structural dynamics: A new modular radial basis function approach vs. convolutional and feedforward topologies, Comput. Methods Appl. Mech. Engrg. 364 (2020) 112989, https://doi.org/10.1016/j.cma.2020.112989.
[23] J.M.P.Q. Delgado, F.A.N. Silva, A.C. Azevedo, D.F. Silva, R.L.B. Campello, R. L. Santos, Artificial neural networks to assess the useful life of reinforced concrete elements deteriorated by accelerated chloride tests, J. Building Eng. 31 (2020) 101445, https://doi.org/10.1016/j.jobe.2020.101445.
[24] M. Kracker, C. Worsch, C. Bocker, C. Rüssel, Optical properties of dewetted thin silver/gold multilayer films on glass substrates, Thin Solid Film. 539 (2013) 47–54, https://doi.org/10.1016/j.tsf.2013.04.153.
[25] Marcin Łapiński, Robert Kozioł, Anita Cymann, Wojciech Sadowski, Barbara Kościelska, Substrate dependence in the formation of Au nanoislands for plasmonic platform application, Plasmonics 15 (2020) 101–107, https://doi.org/10.1007/s11468-019-01021-9.
[26] R. Kozioł, M. Łapiński, P. Syty, D. Koszelow, W. Sadowski, J. Sienkiewicz, B. Kościelska, Evolution of Ag nanostructures created from thin films: UV-vis absorption and its theoretical predictions, Beilstein J. Nanotechnol. 11 (2020) 494–507, https://doi.org/10.3762/bjnano.11.40.
[27] Ivan Nunes da Silva, Danilo Hernane Spatti, Rogerio Andrade Flauzino, Luisa Helena Bartocci Liboni, Silas Franco dos Reis Alves (Eds.), Artificial Neural Networks, Springer International Publishing, Berlin, Germany, 2017.
[28] R. Kozioł, M.S. Łapiński, P. Syty, W. Sadowski, B. Kościelska, Raw Data of AuAg Nanoalloy Plasmon Resonances Used for Machine Learning Method, Gdańsk University Technol. (2021), https://doi.org/10.34808/n560-5948.
[29] D.P. Kingma, J. Ba, Adam: A method for stochastic optimization, 2015.
[30] S. Ozdemir, Principles of Data Science, Packt Publishing (2016).
[31] P. Burman, A comparative study of ordinary cross-validation, v-fold cross-validation and the repeated learning-testing methods, Biometrika 76 (3) (1989) 503–514, https://doi.org/10.2307/2336116.
[32] H. Oh, A. Pyatenko, M. Lee, Laser dewetting behaviors of Ag and Au thin films on glass and Si substrates: Experiments and theoretical considerations, Appl. Surf. Sci. 475 (2019) 740–747, https://doi.org/10.1016/j.apsusc.2019.01.055.
[33] K.L. Kelly, E. Coronado, L.L. Zhao, G.C. Schatz, The Optical Properties of Metal Nanoparticles: The Influence of Size, Shape, and Dielectric Environment, J. Phys. Chem. B. 107 (2003) 668–677, https://doi.org/10.1021/jp026731y.
[34] Masaharu Tsuji, Yuki Nishizawa, Kisei Matsumoto, Nobuhiro Miyamae, Takeshi Tsuji, Xu Zhang, Rapid synthesis of silver nanostructures by using microwave-polyol method with the assistance of Pt seeds and polyvinylpyrrolidone, Colloids Surf., A 293 (2007) 185–194, https://doi.org/10.1016/j.colsurfa.2006.07.027.
[35] D.K. Bhui, H. Bar, P. Sarkar, G.P. Sahoo, S.P. De, A. Misra, Synthesis and UV–vis spectroscopic study of silver nanoparticles in aqueous SDS solution, J. Mol. Liq. 145 (2009) 33–37, https://doi.org/10.1016/j.molliq.2008.11.014.
[36] X. Liu, D. Li, X. Sun, Z. Li, H. Song, H. Jiang, Y. Chen, Tunable Dipole Surface Plasmon Resonances of Silver Nanoparticles by Cladding Dielectric Layers, Sci. Rep. 5 (2015) 12555, https://doi.org/10.1038/srep12555.
[37] Kreibig, U.; Zacharias, P. Z. Phys., Surface plasma resonances in small spherical silver and gold particles, 1970, 231, 128–143, doi.org10.1007/bf01392504.
[38] Florent Calvo, Thermodynamics of nanoalloys, Phys. Chem. Chem. Phys. 17 (2015) 27922–27939, https://doi.org/10.1039/C5CP00274E.
[39] Chao Wang, Sheng Peng, Ryan Chan, Shouheng Sun, Synthesis of AuAg alloy nanoparticles fromcore/shell-structured Ag/Au, Small 5 (2009) 567–570, https://doi.org/10.1002/smll.200801169.
[40] K. Mallik, M. Mandal, N. Pradhan, T. Pal, Seed mediated formation of bimetallic nanoparticles by UV irradiation: a photochemical approach for the preparation of "core-shell" type structures, Nano. Lett. 1 (2001) 6, https://doi.org/10.1021/nl0100264.
[41] S.P. Chenakin, N. Kruse, Au 4f spin–orbit coupling effects in supported gold nanoparticles, Phys. Chem. 18 (2016) 22778–22782, https://doi.org/10.1039/c6cp03362h.
[42] J. Čechal, J. Polčák, T. Šikola, Detachment Limited Kinetics of Gold Diffusion through Ultrathin Oxide Layers, J. Phys. Chem. C 118 (2014) 17549–17555, https://doi.org/10.1021/jp5031703.
[43] B. Balamurugan, T. Maruyama, Size-modified d bands and associated interband absorption of Ag nanoparticles, J. Appl. Phys. 102 (2007), 034306, https://doi.org/10.1063/1.2767837.
[44] Tao Chen, Sha Yang, Jinsong Chai, Yongbo Song, Jiqiang Fan, Bo Rao, Hongting Sheng, Haizhu Yu, Manzhou Zhu, Crystallization-induced emission enhancement: A novel fluorescent Au-Ag bimetallic nanocluster with precise atomic structure, Sci. Adv. 3 (2017), e1700956, https://doi.org/10.1126/sciadv.1700956.
[45] R.E. Watson, J. Hudis, M.L. Perlman, Charge Flow and d Compensation in Gold Alloys, Phys. Rev. B 4 (1971) 4139, https://doi.org/10.1103/PhysRevB.4.4139.
[46] Ji Xiang, Peng Li, Yongbo Song, Xia Liu, Hanbao Chong, Shan Jin, Yong Pei, Xiaoyou Yuan, Manzhou Zhu, X-Ray crystal structure and optical and electrochemical properties of the Au15Ag3(SC6H11)14 nanocluster with a core–shell structure, Nanoscale 7 (2015) 18278–18283, https://doi.org/10.1039/C5NR05131B.
[47] S.J. Pan, Q. Yang, A Survey on Transfer Learning, IEEE Trans. Knowl. Data Eng. 22 (10) (2010) 1345–1359, https://doi.org/10.1109/TKDE.2009.191.